ELSEVIER

Thin Solid Films 412 (2002) 3–13

thin solid films

www.elsevier.com/locate/tsf

Hybrid epitaxial structures for spintronics

J. De Boeck*, W. Van Roy, V. Motsnyi, Z. Liu, K. Dessein, G. Borghs

IMEC, Kapeldreef 75, B-3001 Leuven, Belgium

Abstract

The use of electron spin in future spintronic applications requires hybrid ferromagnetic/semiconductor structures with well controlled materials properties. Besides the control of the magnetic properties there are strict requirements for the material aspects of these devices: single phase, single crystal, perfect interfaces, defect control. Molecular beam epitaxy (MBE) has been used very successfully over the past 10 years to produce the most interesting spintronic heterostructures. In this paper we review our effort in using MBE to fabricate spintronic materials and heterostructures. We also discuss some aspects of future spintronic devices with the focus on the material aspects of transferring the electron spin information from the magnetic side of the heterostructure into the semiconductor side. © 2002 Elsevier Science B.V. All rights reserved.

Keywords: Molecular beam epitaxy; Spintronic materials; Magnetic semiconductors; Spin-injection

1. Introduction

Molecular beam epitaxy (MBE) has proven its strengths in many fields of research and development on (opto-)electronics over the past decades. Spintronics, the field of electronics where the use of the electron spin in semiconductor components is envisaged, is no exception. In order to fabricate devices that intend to combine magnetic and semiconductor properties in very intimate way, the physical combination of the materials is required. One important requirement for spintronic components is the injection of electron spin polarized current into a semiconductor heterostructure, a process mostly referred to as spin-injection. This spin-injection process can be achieved by realizing a magnetic contact on a semiconductor or by the incorporation of some sort of spin-filter. This paper aims to illustrate the strength of MBE in realizing materials combinations that can lead to efficient spin-injection. It is not the ambition to give an exhaustive description of all possible materials combinations, but rather to review some important aspects of spin-source fabrication illustrated with some recent results from our own research activity. In line with today's emphasis to demonstrate the spin-injection process in III–V (electroluminescent) semiconductor devices, the paper will be focused on GaAs based epitaxial heterostructures.

*Corresponding author. Tel.: +32-16-281518; fax: +32-16-281501.

E-mail address: deboeck@imec.be (J. De Boeck).

In the first part of the paper we will describe the epitaxy of metallic ferromagnetic elements and alloys on GaAs. We review some results of initial experiments on Fe and Co epitaxy, since these materials are in the picture for Schottky barrier spin-injection devices today. Further, a brief description of Mn-based alloys will be presented, justified by the wealth of possible Mn-III or Mn-V alloys that can be epitaxially grown on GaAs with various properties. This section is followed by a summary of the results obtained recently on the epitaxial growth of NiMnSb on GaAs, a half-metallic magnetic alloy, that has potential to serve as a spin-source with 100% spin-polarization. We will further briefly discuss some results on the realization of heterostructures including two magnetic layers spaced by a semiconductor or vice versa.

A very appealing class of materials for spintronics is that of magnetic semiconductors, illustrated in this paper by (Al,Ga)MnAs. A concluding section deals with the contact strategies (ohmic, Schottky barrier or tunnel barrier) for spin-injection reports in which where the described materials combinations play an important role.

2. Epitaxy of metallic ferromagnets on semiconductor substrates

2.1. Requirements for good epitaxy

With the continuing downscaling of devices and with the advent of nanoscale devices, the dimensions of, e.g.

0040-6090/02/$ - see front matter
PII: S0040-6090(02)00305-X

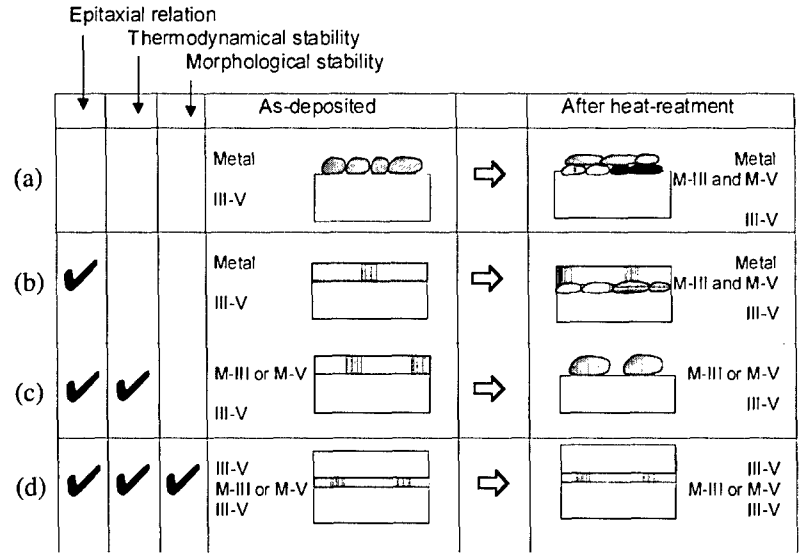

Fig. 1. Schematic representation of the conditions for realizing good epitaxial metal III-V heterostructures.

the metal contacts can be on the order of the grain size of the polycrystalline metals normally used. Although this might not be an important issue for standard electronic devices, it is a very important issue for devices working with the magnetic properties of the metallic contacts. Magnetic properties such as anisotropy and available spin-polarization, e.g. are very closely linked to crystal structure and orientation. MBE enables to realize epitaxial metallic structures with well-controlled crystal orientation and quality.

Epitaxy of metals on semiconductors has been an active area of research over the past two decades. Many successful attempts have been reported to deposit stable, single crystal metallic thin films on semiconductor surfaces. An excellent review of such studies for metal–III–V semiconductor combinations is published by Sands et al. [1]. The items of concern are schematically shown in Fig. 1. We finally want to arrive at a pinhole-free, monocrystalline metal. The interface should remain well defined after possible heat treatment during device fabrication or operation. Eventually, one may attempt to fabricate a metal/semiconductor/metal stack multilayer, in which case the epitaxy criterion is of importance to maintain good quality semiconductor overgrowth.

The result after annealing in conditions A of Fig. 1 is the typical case for a metal contact to a semiconductor structure, in, e.g. MESFET technology. After annealing many phases may form and the metal layer is polycrystalline in nature. In the as-grown condition there is no tendency to form a continuous layer due to the failure to meet the epitaxy criterion.

In case B (Fig. 1), there exists some epitaxial relation to the semiconductor, which helps to stabilize the metal layer. After heat treatment, phase separation occurs due to thermodynamical instability. When meeting both the epitaxy and the thermodynamical criteria, as in case C, the annealing will still cause problems due to insufficient morphological stability. The alloy phase that was deposited epitaxially as grown, will ball up into a highly textured polycrystalline film. Notice that, often metal-III or metal-V alloys have a higher chance to remain thermodynamically stable. In the final case (D), all three criteria are fulfilled and a stable metal/III–V heterostructure results. In this case, semiconductor overgrowth can be attempted with a reasonable chance of success. An example of the latter are GaAs/ErAs/GaAs resonant tunneling structures [2–4] and GaAs/AlAs/NiAl/AlAs/GaAs [5]. In the case of the GaAs/ErAs/GaAs heterostructures [6,7], a negative differential resistance was observed at room temperature for ErAs thicknesses in the range of 2.6–5 nm [8]. The success was attributed to the use of a Mn-template monolayer deposited prior to ErAs deposition.

2.2. Co and Fe epitaxy on GaAs

Fig. 2 shows a set of examples metallic and ferromagnetic structures that have been grown epitaxially on GaAs. The report on epitaxy of Co on GaAs by Prinz [9] is one of the pioneering papers on magnetic/semiconductor epitaxy [10]. Quite some research groups have been very active in the study of epitaxy of elemental magnetic thin films of Co and Fe on GaAs (for a review see also Bland and Heinrich [11]). Such studies have addressed in detail the evolution of the magnetic anisotropy of thin (a few monolayers) Fe [12] and Co films on GaAs. The substrate conditions prior to metal deposition are crucial in the control of this anisotropy since contributions to the net magnetic anisotropy arise from the formation of the interface and

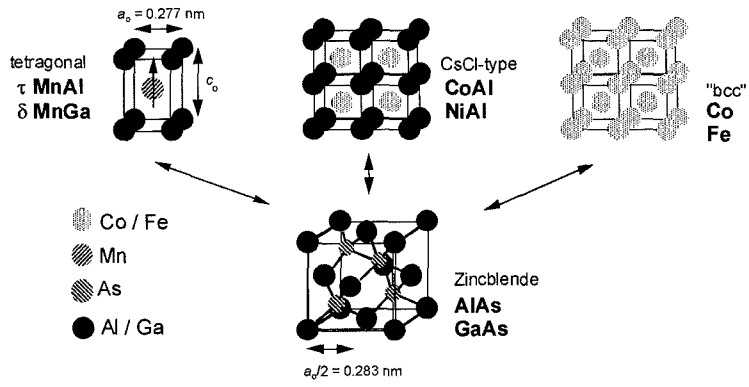

Fig. 2. A set of magnetic materials, well suited for epitaxy on the zinc-blende Ga(Al)As.

early stages of metal film growth. The determining factors are the initial metal adsorption sites and subsequent bond or site filling, and are strongly dependent on the semiconductor surface reconstruction [13,14]. Also, anisotropies can be influenced by surface topography, such as in the case of epitaxy on cross-hatched InGaAs epilayers [15], and by the early stages of the growth (e.g. step bunching and island formation). The domain structure and magnetization reversal processes, dictated by the induced magnetic anisotropy, have been studied in-situ and ex-situ.

In the case of Cobalt epitaxy on GaAs a forced phase [16] of Co, the bcc phase [9], can be realized due to the epitaxial relationship. A review of the bcc Co related work until 1991 was given by Prinz [17]. More recently the study of bcc Co as seed layers for epitaxial metal structures on GaAs has been reported, as well as further studies on the structural [18] and magnetic properties [19] of bcc Co and CoFe alloys [20]. The appearance of bcc Co in superlattices of Co/Fe [21–23], Co/Pd(111) [24] and Co/τ-MnAl [25] has been demonstrated. In the case of the Co/Fe superlattices, nuclear magnetic resonance (NMR) measurements on the short range chemical order in combination with hyperfine field experiments have illustrated the limits of stability. In superlattices with Co thicknesses above 2 nm, alloy formation with Fe at the interfaces is responsible for the observation of the bcc phase. From reflection high energy electron diffraction (RHEED) during the growth of the Co, it was concluded that the bcc phase is not sustained beyond approximately 1 nm.

2.3. Epitaxial Mn-based alloys on GaAs

When a metal alloy contains either a group III or a group V element, good interface characteristics can be expected. MnAs is such an alloy, that has been grown epitaxially on GaAs [26–28], for which it was shown that the preparation of the semiconductor surface before growth changes the orientation of the epilayer with respect to the crystal orientation of the substrate. Another example of this class is MnSb epitaxy which has been demonstrated recently [29,30]. As in the case of elemental metals, the magnetization of these epitaxially grown alloys is in the plane of the film. Another interesting class of epitaxial magnetic films is that of Mn-III alloys, in which the magnetization is out of the plane. Examples of this class are Mn-based magnetic thin films such as τ MnAl [31,32] and δ MnGa [33,34] (see Fig. 2). In these cases, the epitaxial growth on a III–V semiconductor substrate (such as GaAs) is the key to obtaining the desired perpendicular magnetization. The metastable phase τ MnAl can be stabilized by coherence to the semiconductor substrate and due to the epitaxial relationship, the *c*-axis of the tetragonal lattice is normal to the growth surface. As a consequence, the easy axis of the magnetization of the thin film points out of plane. The flexibility in engineering new epitaxial multilayers and new magnetic properties using this class of ferromagnetic films have been demonstrated: MnGa/NiGa [35] which multi-stepped hysteresis loops and ferrimagnetic τ MnAl/Co superlattices on GaAs [36–38], in which both magnetic sub-layers of the superlattice have a perpendicular magnetization, which are aligned anti-parallel at zero field. Very large antiferromagnetic interface coupling strength is observed, together with a strong perpendicular magnetic anisotropy for both the τ MnAl and the Co layers. Kerr hysteresis loops of τ MnAl/Co superlattices show abrupt transitions from anti-aligned to aligned states. The Co layers are found to be partially in the bcc phase.

In alloys like MnAl and MnGa, a large imbalance in density of states for majority and minority spins exists approximately 1 eV above the Fermi-level [39,40]. This property makes them interesting for ballistic magneto-transport studies in ferromagnet/semiconductor hybrid devices.

2.4. Epitaxial half-metallic ferromagnets

Even if one can realize perfect epitaxial metallic ferromagnets on a semiconductor, these structures will

always suffer from the disadvantage that there is not a 100% polarization in the magnetic contact. Metallic ferromagnetic contacts have, at best, a polarization on the order of 40%. The spintronic device performance will be enhanced greatly, as described in more detail in the final section of this paper, when the spin-source for the device is polarized a full 100%. Such a situation occurs in half metallic ferromagnets, of which NiMnSb is one example which has been shown theoretically [41,42] and experimentally [43] to be half-metallic in the bulk. It has the interesting property that it meets the criteria to be grown epitaxially on GaAs [44]. The NiMnSb/GaAs combination is an excellent candidate for atomically controlled interfaces because its crystal structure is very closely related to the zinc-blende structure of III–V semiconductors [44]. With a bulk lattice constant [45] of 5.903 Å, NiMnSb shows a mismatch of 4.4% with GaAs ($c=5.6533$ Å). Our samples, typically consisting of a 200 nm GaAs buffer and 260–350-nm-thick NiMnSb films, were grown with a base pressure of less than 1×10^{-10} torr on either GaAs (001) or (111) [46]. The growth was initiated by simple co-evaporation of all three elements, i.e. no attempt was made to control the nucleation of NiMnSb on a particular plane in the initial experiments.

On GaAs (100), the best morphology was obtained at a substrate temperature of approximately 300 °C, where the RHEED patterns remained streaky throughout the entire growth. The stoichiometry of the films depended strongly on the Sb flux. Fig. 3 shows the Sb content x_{Sb} of NiMnSb 1:1:x_{Sb} films grown with an Sb BEP flux $\phi Sb=5\sim13\times\phi Ni$, as measured by Rutherford back-scattering (RBS). In contrast to the growth of III–V semiconductors, there is no self-limiting mechanism for the incorporation of the group-V element. Rather, there is an optimum flux ratio $\phi Sb=10\times\phi Ni$ where stoichiometric films are obtained. Films grown with lower Sb flux are Sb deficient, while films grown at higher flux contain excess Sb. The total film thickness reflects these changes in Sb incorporation (Fig. 3b, determined by RBS).

All films grew in the (001) orientation as measured by XRD. Stoichiometric films showed a lattice constant c of 5.904–5.909 Å that is almost identical to the bulk lattice constant, while non-stoichiometric films, especially on the Sb-poor side, showed deviations, as indicated in Fig. 3c. NMR studies were performed on these films [47].

The room-temperature magnetization Ms shown in Fig. 3d correlates well with the structural properties of the films. Stoichiometric films have Ms of 450–570 kA/m slightly below the bulk value 720 kA/m and a coercive field, H_c of 2–4 mT. In addition, stoichiometric films show a varying degree of in-plane uniaxial anisotropy with the easy axis along ⟨110⟩ or ⟨1−10⟩ depending on the growth conditions and on the choice of

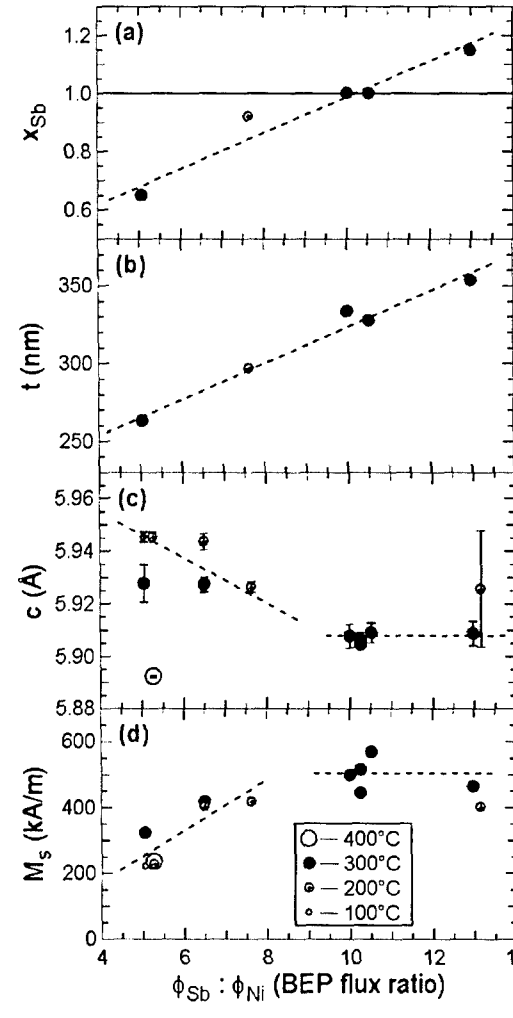

Fig. 3. Variations of the thin film properties of NiMnSb epitaxially grown on GaAs (001) with the variation of the Ni to Sb beam equivalent pressure.

interface layer. We are currently investigating the spin-polarization at the interface of the NiMnSb and GaAs/AlGaAs heterostructures by optical assessment of the spin-injection.

Although there are many other candidates for half-metallic ferromagnetic contacts, such as Cr_2O with measured polarization of 96% and above [48], they all face the challenge to preserve the half-metallicity down to the injection interface, in addition to be stable and structurally compatible with the underlying semiconductor.

2.5. SC/FM/SC and FM/SC/FM heterostructures

As the technology of building artificial structures improves, even more challenging structures may become possible such as epitaxial multilayers of magnetic metal and semiconductors (case D in Fig. 1). Van Roy et al. reported magnetoresistance and coupling effects as a function of the (Ga,Mn,As) thickness in MnGa/

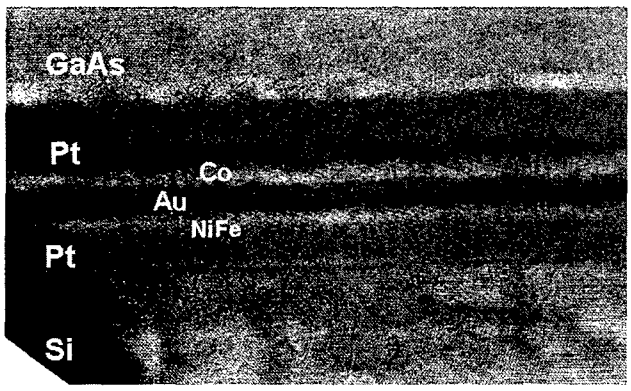

Fig. 4. A TEM cross-section of a GaAs/spin-valve/Si spin-valve transistor.

(Ga,Mn,As)/MnGa trilayers [49]. When such structures are further optimized, control of magnetic properties with external modulation sources such as optical power, may become reality. Butler et al. have performed calculations of the electronic structure of an Fe/GaAs/Fe structure. They conclude that the simple models relying on potential barriers or density of states from the bulk may not apply to such FM/SC/FM structure [50].

Magneto-optical properties of Co(100)/Ge/Co trilayers have been reported [51]. The coercivity and the anisotropy of these structures oscillate with the Ge thickness. CoPt/(Si, Ge)/Co trilayer and multilayer structures have been fabricated and analyzed using CPP magnetotransport [52]. In these structures a small steep CPP resistance change has been found that was ascribed to the change in the relative spin orientation of the Co (magnetic soft) and the CoP (magnetic hard) layers.

Although these structures show promising results, often stability at higher temperatures (even room temperature) is a critical issue.

One interesting example of a semiconductor/ferromagnetic/semiconductor is that of the spin-valve transistor (SVT) [53,54]. This device is a metal base transistor with a semiconductor emitter (either Si of GaAs) and a semiconductor collector (Si) in which the metal base is replaced by a spin-valve multilayer. Dessein et al. have succeeded in making a GaAs/SV/Si version of the SVT [55] in which MBE has played a crucial role for the fabrication of the Ga(Al)As emitter structure. The SVT device is fabricated by a room-temperature vacuum wafer bonding technique: two clean and smooth semiconductor substrates are brought into contact during the evaporation of the magnetic multilayer. The resulting bond is of very high structural and electrical quality. This is illustrated by Figs. 4 and 5. Fig. 4 shows a transmission electron microscopy (TEM) cross-section of the finished GaAs/Spin-valve/Si SVT. The magnetotransport characteristic in Fig. 5 illustrates the functionality of the device [56].

3. GaMnAs ferromagnetic semiconductor

3.1. Low-temperature MBE for GaMnAs

Although magnetic (half-)metallic materials offer great potential as contacts in hybrid spintronic devices, they do not offer any flexibility in terms of modulating their degree of spin-polarization. It would be nice to have a magnetic material that is fully compatible with a major class of semiconductors and that offers the possibility to change its ferromagnetic properties with light, voltage, current. Ferromagnetic semiconductors have that potential, in particular the ferromagnetic semiconductors that are based on GaAs and GaN III–V semiconductors. The most studied of this family is GaMnAs, in which a high concentration of Mn is incorporated in the zinc-blende lattice of the GaAs host. Again, MBE plays the leading role in the development of this material because of the need for growing the highly supersaturated GaMnAs far out of equilibrium conditions. The success in GaMnAs ferromagnetic material was initiated by the use of a low-temperature growth procedure [57,58]. Growth at such a low temperature is made necessary by the fact that at higher temperatures there is a tendency to form ferromagnetic MnAs precipitates within the GaMnAs alloy [59]. However, the low temperature necessary for such precipitate-free growth also results in the formation of As antisites that form deep levels, counteracting the effectiveness of the Mn^{2+} acceptors through compensation. Parameters such as temperature, relative cation fluxes and As overpressure play an important role in the quality of the final layer characterized often by the (critical-) paramagnetic-ferromagnetic transition temperature T_c. Efforts to optimize the incorporation of Mn into the III–V lattice have led to controversial statements [60,61] but good results

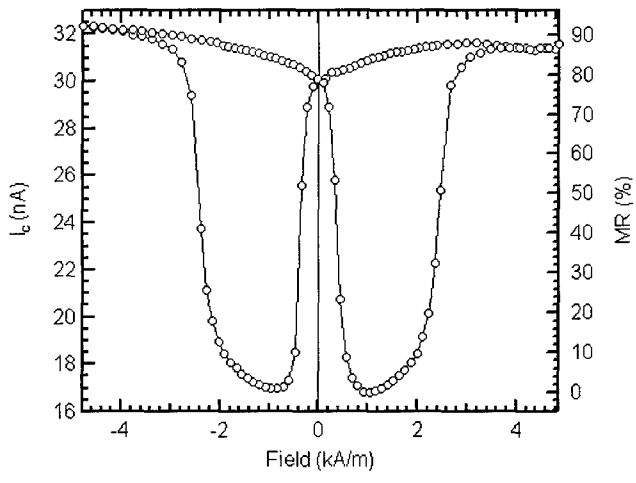

Fig. 5. The magnetocurrent characteristics of an optimized GaAs-spin-valve transistor.

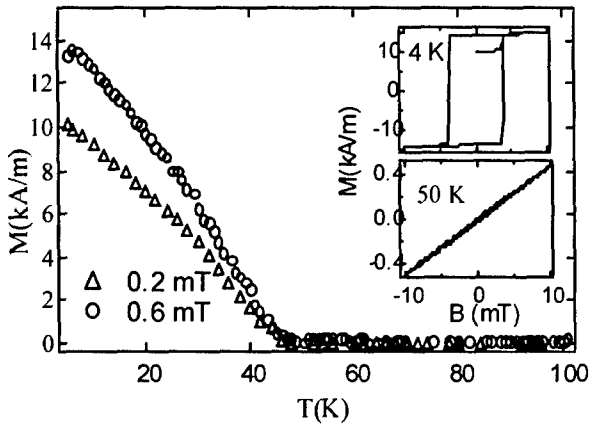

Fig. 6. SQUID magnetization measurements show the onset of magnetic ordering at $T_c = 45$ K. The insets show the hysteresis measured at $T = 4$ K with the field parallel to the surface and the paramagnetic signal at 50 K.

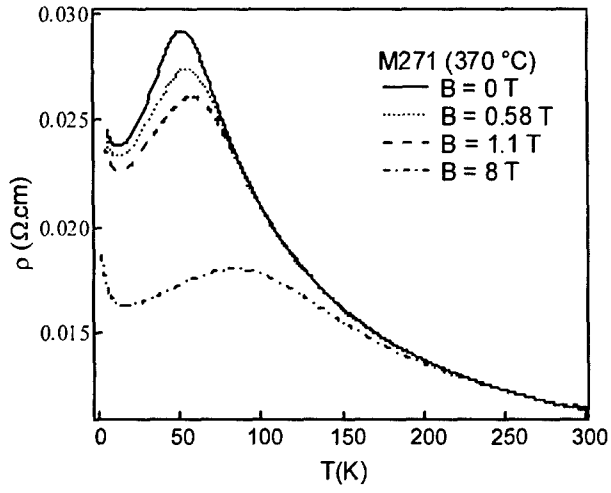

Fig. 7. Temperature dependence of the resistivity of Ga0.93Mn0.07As in a constant applied field of 0.58 T, 1.1 T and 8 T.

have been obtained by different groups and a T_c reaching 110 K has been reported [62].

3.2. The ferromagnetic properties of GaMnAs

The ferromagnetism of $III_{1-x}Mn_xAs$ alloys originates from two ingredients: the obvious presence of magnetic ions in the form of Mn^{2+} and the high concentration of holes in these systems, also supplied by the Mn^{2+} ion, which acts as an acceptor when substituted into the III–V lattice. The ferromagnetism of III–Mn-V as well as trends in the observed T_c have been explained by carrier-induced ferromagnetism in which uniform itinerant-carrier spin polarization mediates a long-range ferromagnetic interaction between the Mn^{2+} ions with spin 5/2 [63]. As was shown recently [64], the mean field theory based on the RKKY interaction has only limited validity, and although it can provide a realistic estimate of T_c it fails as a theory of the ferromagnetic state. It lacks dynamic correlations in the localized and itinerant spin system.

The most striking magnetic property of $III_{1-x}Mn_xV$ alloys is of course their ferromagnetic behavior below the Curie temperature. A characteristic hysteresis loop is demonstrated in the inset of Fig. 6.

3.3. Electronic properties of GaMnAs

Quantitative measurements of saturation magnetization Ms result in values close to the calculated value $N_{Mn}g\mu_bS$. However, annealing experiments have revealed that this value strongly depends on temperature during or after growth. Mn–As complexes can be formed during annealing, different from MnAs precipitates formed at higher temperatures. Also the number of holes for a given Mn concentration x can be maximized during growth by optimizing the growth parameters so as to reduce the As antisites.

Hole concentrations in magnetic semiconductors are determined from Hall effect measurements but an accurate measurement is often troublesome, if possible at all, due to the contribution of the extra-ordinary Hall effect term. Moreover, the negative magnetoresistance effect and, at very low temperature, the contribution of a hopping component to the carrier transport further complicate the measurements.

According to Oiwa et al. [65] the magnetoelectronic states can be divided into three concentration regions: samples in the region $0.01 < x < 0.03$ are ferromagnetic but insulating (i.e. their resistivity increases dramatically with decreasing temperature; those in the range $0.03 < x < 0.06$ are metallic (i.e. their resistivity below T_c is approximately independent of temperature); and those samples with Mn concentration in the range above 0.06 again showing insulating behavior, most probably due to increased disorder of magnetic and coulombic nature. It is also striking that the metallic samples have the highest values of the Curie temperature.

For a given x there is an almost direct proportionality between the hole concentration p and the corresponding value of the Curie temperature, up to a value of almost $x = 0.06$ beyond which T_c drops again. The typical hole concentration is 20% below the Mn concentration due to compensation [62].

From the magnetic properties of GaMnAs it is clear that holes have a direct and decisive effect on the behavior of the system. It is not surprising that the inverse is also true: transport properties of the alloys are strongly linked to their magnetic character. One interesting feature common to these materials is that $\rho(T)$ displays a peak at the Curie temperature, that is assumed to arise from enhanced spin scattering as one passes

through the critical temperature as shown in Fig. 7 where temperature sweeps of the resistivity of different $Ga_{1-x}Mn_xAs$ layers in a constant field of 0.58 T, 1.1 T and 8 T are given.

The temperature dependence of the resistivity can be interpreted as critical scattering by packets of magnetic spins with ferromagnetic short-range order characterized by the correlation length comparable with the wavelength of the carriers at the Fermi level [66]. In addition to critical scattering, alloys in the insulating regime also display an enormous negative magnetoresistance occurring at low temperatures, but even at temperatures above the critical temperature also shown in Fig. 7. Both rapid rise of the resistivity with decreasing temperature in the insulating samples, and its dramatic drop with magnetic field at cryogenic temperatures can be understood in terms of magnetic polarons. Magnetic polarons, which form continuously as the temperature decreases, are extremely efficient scatterers, thus accounting for the rise of resistivity. Application of a magnetic field destroys the polarons, restoring the resistivity to what it would have been in their absence.

The application of Mott's concept of a mobility edge, the formation of polarons and the localization in a magnetic system with coulomb disorder was used to describe the metal insulator transition in a magnetic semiconductor [67].

This transition, as well as the negative magnetoresistance is contrary to non-magnetic heavily doped semiconductors where a positive magnetoresistance results from a shrinkage of impurity states orbits in high applied fields. Localization occurs now because of the combined action of random potential fluctuations and the magnetic disorder.

The magnetic properties of diluted magnetic II–VI (and IV–VI) semiconductors have been studied theoretically in great detail and many results are applicable to the III–V materials as well, the important difference being the nature of the Mn impurity atom itself. The magnetic ion which occupies the cation (Ga) sublattice in zinc-blende GaMnAs provides a localized spin and at the same time act as an acceptor. Despite the strong doping compensation, all III–V Mn materials are heavily doped p^+.

Undoped II–VI magnetic semiconductors show a spin-glass transition at low temperature due to the direct antiferromagnetic coupling between Mn ions. Upon doping, the transition from a spin-glass antiferromagnetic to a ferromagnetic phase happens and is caused by a RKKY interaction between free carriers and localized Mn spins. A corresponding change in Curie temperature from negative to positive occurs and was first discovered in IV–VI materials by Story et al. [68].

It can be shown [69] that the critical temperature derived from the RKKY interaction, with the approximations made, compares well with that derived from a total low-field magnetic susceptibility of the coupled system of carriers and localized spins in the mean field approximation. This important conclusion justified the application of the mean field theory in GaMnAs and according to Dietl et al. [63] this model has its origin in one originally proposed by Zener [70] in an early attempt to explain ferromagnetism in transition metals. This semi-empirical approach allows to include e.g. spin-orbit splitting, the effect of strain and heavy doping effects based on carrier–carrier interactions and is able to explain quantitatively the Curie temperature Tc of GaMnAs (and ZnMnTe doped with nitrogen) and the influence of strain on the orientation of the magnetization.

The complex valence-band structure of zinc-blende ferromagnetic semiconductors was included in the theoretical model based on the mean field theory for hole mediated exchange. It was found that spin-orbit coupling had an important effect on the Curie temperature and the direction of the magnetization below T_c. Higher values for T_c are predicted for materials containing larger concentrations of holes and magnetic ions and for zinc-blende structures with lighter elements like GaN but also ZnO.

3.4. AlMnAs: a new magnetic semiconductor

With the intention to fabricate heterostructures in which modulation doping or spin-filtering will become possible, we studied the growth of $Al_{1-x}Mn_xAs$ with up to 4% Mn. Stoichiometric low-temperature MBE conditions are achieved by using an As_4 flux at the Ga-rich-to-As-rich growth boundary. The samples were grown on a GaAs(100) substrate at 230 °C. The two-dimensional growth as the dominating process is verified by clearly observed RHEED oscillations and streaky (1×2) patterns during growth. Structural characterization with XRD reveals crystal quality comparable to GaMnAs. The change of the lattice constant of AlMnAs is roughly proportional to the Mn flux, suggesting complete incorporation of Mn atoms.

Fig. 8 illustrates the magnetization measurements on (a) $Al_{0.97}Mn_{0.03}As$ and (b) $Al_{0.96}Mn_{0.04}As$. These indicate that the 3% Mn sample follows the Brillouin function quite nicely and shows no ferromagnetic behavior, while the 4% Mn sample shows a ferromagnetic signal at low temperatures. The ferromagnetic signal is ascribed to the presence of nanometer-scale magnetic particles formed in the AlMnAs layer, most likely MnAs. AlMnAs layers were then incorporated in heterostructures. One interesting heterostructure is AlMnAs/δ-Mn/GaAs where a 2DHG is formed at the AlMnAs/GaAs interface. Below the transition temperature of the AlMnAs, in this case 10 K, we found evidence of a strong interaction between the magnetic moments near the interface and the 2DHG. This interaction is visible in

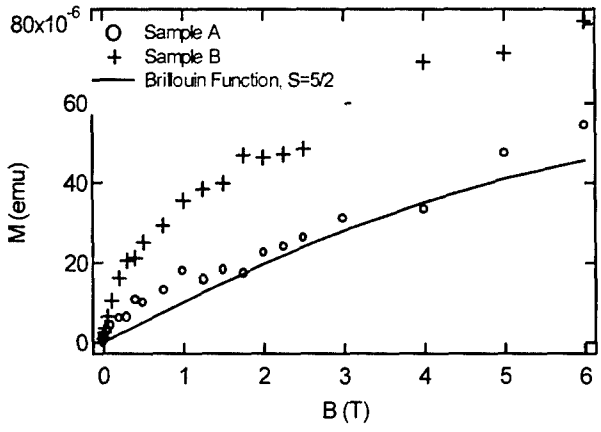

Fig. 8. SQUID magnetization measurements of AlMnAs layers with (a) 3% and (b) 4% Mn.

the Hall-effect measurements. These observations will be published elsewhere [71].

4. Spin-injection device trials

In order to demonstrate a spintronic effect, existing semiconductor devices are mimicked using a combination of magnetic and semiconductor materials. Examples are: the spin-FET [72], where magnetic source and drain are used in a field-effect transistor layout, the hot-electron metal-base transistor, the spin-valve transistor [53], where a magnetic multilayer is replacing the metal base, and light-emitting devices [73,74]. It is important to realize that for all such attempts, the spintronic device will not deliver the same functionality or the same performance as the original semiconductor device. It would be a mistake to believe that a well-known transistor structure could be turned into an improved version by making it function with electron spins rather than charge. In the best case they illustrate a novel, magnetic functionality and/or show the effect of spin transport. Their importance lies in the fact that with the fabrication of such novel 'transistors' the complexity of the magnetic/semiconductor materials combination is revealed and our understanding of spin-transport improves.

4.1. Ohmic or tunnel contact?

Let's concentrate on the efforts of injecting a spin-polarized current in a semiconductor from a metallic magnetic contact. Many attempts have been made to fabricate such a spin-injection structure using an ohmic contact. It was recently described [75] why such attempts are unsuccessful [76,77] when the ferromagnetic and the semiconductor are in the diffusive contact regime. The effectiveness of spin-injection from the ferromagnetic is reduced by a factor M expressing the mismatch in conductivity and spin-flip length between the two materials:

$$M = 1 + \frac{\sigma_F}{\sigma_N}\frac{\lambda_N}{\lambda_F}(1-\alpha_F^2)$$

$$\alpha_F = \frac{\sigma_\uparrow - \sigma_\downarrow}{\sigma_\uparrow + \sigma_\downarrow}$$

is the bulk polarization of the electrodes, $\sigma_{(\downarrow\uparrow)}$ are the spin up (down) conductivities, σ_N (σ_F) is the total conductivity in the semiconductor (ferromagnetic metal) and λ_N (λ_F) is the spin flip length in the semiconductor (ferromagnetic metal). For metallic ferromagnets the value of M is on the order of 100, effectively suppressing the spin-injection [77].

In most cases, however, the metal semiconductor contact will not be a clean ohmic contact. The interface properties will change the electrical behavior of the metal/semiconductor heterostructure. These electrical characteristics are normally designed by changing the electronic properties of the semiconductor using doping and band-gap engineering such that a tunnel barrier, an ohmic contact, or a Schottky barrier is formed. An uncontrolled interface due to phase separation or severe intermixing leads to unpredictable changes in the device performance. The structural and magnetic information on the ferromagnetic/semiconductor interface is quite substantial, but detailed electrical characterization is rather limited. For spin-injection there is recent consensus based on experimental and theoretical [78] results that a tunnel injector is the best alternative. In spin-injection using tunneling, vacuum barriers [79–81], Al_2O_3 barriers [82,83] and Schottky barriers [84,85] have been used. From a device perspective, the vacuum barrier is not very practical and the Schottky barrier might not be very stable. Our preference goes to the fabrication of a stable Al_2O_3 oxide barrier such as used in magnetic tunnel junctions [86–88].

4.2. Al_2O_3: a good tunnel barrier for spin-injection

We recently applied our expertise in fabricating magnetic tunnel junctions to the fabrication of spin-injection structures for realizing spin-injection components. The advantages of this approach are that the magnetic properties of the contact can be well controlled at the metal/insulator interface, and this interface will be more stable over time and with temperature than direct metal/semiconductor heterostructures. Although a Schottky barrier contact can act as a tunnel injector, recent reports show 2% spin injection efficiency at room temperature [84], such devices may suffer from the above stated problems. The fabrication of the tunnel-injector includes the epitaxial growth of a semiconductor heterostructure that should allow the observation of spin-injection. Since the spin-injection efficiency will be assessed through the optical response of the structure, surface emitting

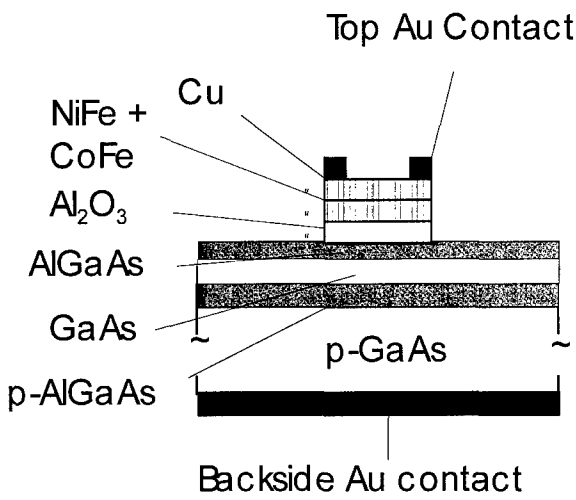

Fig. 9. Schematic cross-section of an LED structure with Al_2O_3 tunnel barrier injector.

LED components were fabricated (see Fig. 9). GaAs/AlGaAs heterostructures were grown by MBE consisting of the active region, interface control, carrier confinement and contact layers for good LED operation. The sample was unloaded from the MBE and transferred to the sputtering tool to fabricate a 1.9-nm-thick Al_2O_3 layer. First an Al layer was deposited which was subsequently oxidized in a controlled O_2 ambient of 100 torr. As a magnetic top contact we sputtered NiFe or CoFe layers. The I–V characteristic show that the tunnel-injector allows to inject electrons in the conduction band of the GaAs active region of the LED. The structure of the Al_2O_3 was not optimized and first attempts were made to deposit the Al for the barrier in the MBE system, without success so far. Using an appropriate optical assessment technique [89] we recently found evidence of spin injection exceeding 8% at 80 K using this type of LED. This is a promising development that may find further improvement if the barrier structure can be optimized, possibly using a full epitaxial structure. The advantage of the oxide barrier approach for the tunneling is, furthermore, that Si-based spintronic structures become possible.

Besides the use of the magnetic contacts to realize spin-injection, moderate spin-injection efficiencies have been obtained using GaMnAs as a spin-injector [74]. The possibility to incorporate the ferromagnetic semiconductors in tunnel structures [90], 2-DEG structures [71] and Schottky barriers [91] and to control the magnetism with voltage [92], makes them highly attractive for future spintronic components. Recent reports on the spin-polarized tunneling from the valence band of GaMnAs to the conduction band of GaAs in a p+-GaMnAs/n+GaAs reverse biased Esaki-type diode [93,94] brings another degree of freedom to the design of FMS-based semiconductor structures.

5. Conclusion

Molecular beam epitaxy is an extremely powerful tool for the exploration of new devices, as proven once more in the field of spintronics. Through the expertise gained in the epitaxy of magnetic thin films on semiconductors and the realization of magnetic semiconductor materials, the progress in spintronic devices using III–V heterostructures has been rapid over the past few years. This paper has highlighted a few areas of research and some of the basic challenges for realizing spin-transport devices.

Acknowledgments

The authors gratefully acknowledge the collaboration with A. Kumar, R. Jansen, R. Vlutters and C. Lodder on the spin-valve transistor; with A. Filip and B. van Wees on the spin injection, with A. Twardowski on the Squid measurements on AlMnAs. Professor V.I. Safarov is acknowledged for his contribution in the assessment of the spin-injection of the tunnel-barrier device [89]. We further thank W. van de Graaf for III-V MBE growth. Parts of this work was funded under the EC contracts: SPIDER, FENIKS (G5RD—CT2001—00535) and SPINOSA. KD acknowledges financial support from the I.W.T. (Belgium). W.V.R. acknowledges financial support as a Postdoctoral Fellow of the Fund for Scientific Research Flanders-Belgium (F.W.O.).

References

[1] T. Sands, C.J. Palmstrøm, J.P. Harbison, V.G. Keramidas, N. Tabatabaie, T.L. Cheeks, R. Ramesh, Y. Silverberg, Mater. Sci. Rep. 5 (1990) 99–170.
[2] J.G. Zhu, C.B. Carter, C.J. Palmstrom, K.C. Garrison, Appl. Phys. Lett. 55 (1990) 39.
[3] J.G. Zhu, C.J. Palmstrøm, C.B. Carter, J. Appl. Phys. 77 (1995) 4312–4320.
[4] D.E. Brehmer, K. Zhang, C.J. Schwarz, S.-P. Chau, S.J. Allen, J.P. Ibbetson, J.P. Zhang, C.J. Palmstrom, Appl. Phys. Lett. 67 (1995) 1268.
[5] T. Sands, J.P. Harbison, N. Tabatabaie, W.K. Chan, H.L. Gilchrist, T.L. Cheeks, L.T. Florez, V.G. Keramidas, Surf. Sci. 228 (1990) 1–8.
[6] S.J. Allen, N. Tabatabaie, C.J. Palmstrom, G.W. Hull, T. Sands, F. DeRosa, H.L. Gilchrist, K.C. Garrison, Phys. Rev. Lett. 62 (1989) 2309.
[7] J.G. Zhu, C.B. Carter, C.J. Palmstrom, S. Mounier, Appl. Phys. Lett. 56 (1990) 1323.
[8] M. Tanaka, M. Tsuda, T. Nishinaga, C.J. Palmstrøm, Appl. Phys. Lett. 68 (1996) 84–86.
[9] G.A. Prinz, Phys. Rev. Lett. 54 (1985) 1051–1054.
[10] G.A. Prinz, Science 250 (1990) 1092.
[11] J.A.C. Bland, B. Heinrich (Eds.), Ultrathin Magnetic Structures, I and II, Springer), Berlin, 1994.
[12] M. Gester, C. Daboo, R.J. Hicken, S. Gray, A. Ercole, J.A.C. Bland, J. Appl. Phys. 80 (1996) 347.
[13] B.T. Jonker, H. Abad, J.J. Krebs, J. Appl. Phys. 76 (1994) 6294.

[14] E. Kneedler, P.M. Thibado, B.T. Jonker, B.R. Bennet, B.V. Shanabrook, R.J. Wagner, L.J. Whitman, J. Vac. Sci. Technol. 14 (1996) 3193.
[15] J.M. Florczak, P.J. Ryan, J.N. Kuznia, A.M. Wowchak, P.I. Cohen, R.M. White, G.A. Prinz, E.D. Dahlberg, Mater. Res. Soc. Symp. Proc. 300 (1989) 213.
[16] A.Y. Liu, D.J. Singh, J. Appl. Phys. 73 (1993) 6189–6191.
[17] G.A. Prinz, J. Magn. Magn. Mater. 100 (1991) 469.
[18] S.J. Blundell, M. Gester, J.A.C. Bland, C. Daboo, E. Gu, M.J. Baird, A.J.R. Ives, J. Appl. Phys. 73 (1993) 5948.
[19] J.A.C. Bland, R.D. Bateson, P.C. Riedi, R.G. Graham, H.J. Lauter, J. Penfold, C. Schackleton, J. Appl. Phys. 69 (1991) 4989.
[20] C.J. Gutierrez, J.J. Krebs, G.A. Prinz, Appl. Phys. Lett. 61 (1992) 2476.
[21] C.J. Gutierrez, J.J. Krebs, M.E. Filipkowski, V.G. Harris, W.T. Elam, J. Magn. Magn. Mater. 126 (1993) 232.
[22] J. Dekoster, E. Jedryka, C. Meny, G. Langouche, J. Magn. Magn. Mater. 121 (1993) 69.
[23] J.P. Jay, E. Jedryka, M. Wojcik, G. Langouche, P. Panissod, Zeit. Physik B 101 (1996) 329.
[24] C.D. England, B.N. Engel, C.M. Falco, J. Appl. Phys. 69 (1991) 5310.
[25] J. De Boeck, W. Van Roy, C. Bruynseraede, A. Van Esch, H. Bender, G. Borghs, Microelectronics J. 27 (1996) 383–392.
[26] M. Tanaka, J.P. Harbison, M.C. Park, Y.S. Park, T. Shin, G.M. Rothberg, J. Appl. Phys. 76 (1994) 6278–6280.
[27] M. Tanaka, J.P. Harbison, G.M. Rothberg, J. Cryst. Growth 150 (1995) 1132–1138.
[28] M. Wojcik, E. Jedryka, S. Nadolski, Z. Liu, K. Dessein, G. Borghs, J. De Boeck, J. Magn. Magn. Mater. 226-230 (2001) 1588–1590.
[29] H. Akinaga, K. Tanaka, K. Ando, T. Katayama, J. Cryst. Growth 150 (1995) 1144–1149.
[30] H. Akinaga, S. Miyanishi, W. Van Roy, L.H. Kuo, Appl. Phys. Lett. 70 (1997) 2472–2474.
[31] T. Sands, J.P. Harbison, M.L. Leadbeater, S.J. Allen, G.W. Hull, R. Ramesh, V.G. Keramidas, Appl. Phys. Lett. 57 (1990) 2609–2611.
[32] W. Van Roy, J. De Boeck, H. Bender, C. Bruynseraede, A. Van Esch, G. Borghs, J. Appl. Phys. 78 (1995) 398–404.
[33] M. Tanaka, J.P. Harbison, J. De Boeck, T. Sands, B. Philips, T.L. Cheeks, V.G. Keramidas, Appl. Phys. Lett. 62 (1993) 1565–1567.
[34] K.M. Krishnan, Appl. Phys. Lett. 61 (1992) 2365–2367.
[35] M. Tanaka, J.P. Harbison, T. Sands, B. Philips, T.L. Cheeks, J. De Boeck, L.T. Florez, V.G. Keramidas, Appl. Phys. Lett. 63 (1993) 696–698.
[36] C. Bruynseraede, J. De Boeck, W. Van Roy, G. Lauhoff, H. Bender, A. Van Esch, R. Mertens, J.A.C. Bland, G. Borghs, MRS Symp. Proc. 384 (1995) 85–90.
[37] G. Lauhoff, C. Bruynseraede, J. De Boeck, W. Van Roy, J.A.C. Bland, G. Borghs, Phys. Rev. Lett. 79 (1997) 5290.
[38] J. De Boeck, C. Bruynseraede, H. Bender, A. Van Esch, W. Van Roy, G. Borghs, J. Cryst. Growth 150 (1995) 1139.
[39] H. Van Leuken, A. Lodder, M.T. Czyzyk, F. Springelkamp, R.A. de Groot, Phys. Rev. B 41 (1990) 5613–5626.
[40] A. Sakuma, J. Phys. Soc. Jpn. 63 (1994) 1422–1428.
[41] R.A. de Groot, F.M. Mueller, P.G. van Engen, K.H.J. Buschow, Phys. Rev. Lett. 50 (1983) 2024–2027.
[42] K.E.H.M. Hanssen, P.E. Mijnarends, Phys. Rev. B 34 (1986) 5009–5016.
[43] K.E.H.M. Hanssen, P.E. Mijnarends, L.P.L.M. Rabou, K.H.J. Buschow, Phys. Rev. B 42 (1990) 1533–1540.
[44] W. Van Roy, J. De Boeck, B. Brijs, G. Borghs, Appl. Phys. Lett. 77 (2000) 4190–4192.
[45] L. Castelliz, Z. Metallkde 46 (1955) 201.
[46] W. Van Roy, M. Wojcik, E. Jedryka, S. Nadolski, O. Richard, B. Brijs, G. Borghs, J. De Boeck, JEMS 01, Grenoble, France (2001) to be presented.
[47] M. Wojcik, E. Jedryka, S. Nadolski, W. Van Roy, G. Borghs, J. De Boeck@ J. Magn. Magn. Mater. (2001) submitted.
[48] Y. Ji, G.J. Strijkers, F.Y. Yang, C.L. Chien, J.M. Byers, A. Anguelouch, Xiao Gang, A. Gupta, Phys. Rev. Lett. 86 (2001) 5585.
[49] W. Van Roy, H. Akinaga, S. Miyanishi, K. Tanaka, L.H. Kuo, Appl. Phys. Lett. 69 (1996) 711.
[50] W.H. Butler, X.-G. Zhang, X. Wang, J. van Eck, J.M. MacLaren, J. Appl. Phys. 81 (1997) 5518.
[51] S.S. Kang, G.J. Jin, X.N. Xu, H.R. Zhai, S.S. Jiang, Y. Chen, W.R. Zhu, G.S. Dong, S.M. Zhou, X. Jin, J.W. Feng, Appl. Phys. Lett. 69 (1996) 3923–3925.
[52] K. Matsuyama, H. Asada, T. Saeki, Y. Sawamoto, K. Tanaguchi, J. Appl. Phys. 51 (1997) 5449.
[53] D.J. Monsma, J.C. Lodder, T.J.A. Popma, B. Dieny, Phys. Rev. Lett. 74 (1995) 5260–5263.
[54] D.J. Monsma, R. Vlutters, J.C. Lodder, Science 281 (1998) 407–409.
[55] K. Dessein, H. Boeve, P.S.A. Kumar, J. De Boeck, J.C. Lodder, L. Delaey, G. Borghs, J. Appl. Phys. 87 (2000) 5155–5157.
[56] K. Dessein, A.P.S. Kumar, L. Lagae, J. De Boeck, L. Delay, G. Borghs, J. Magn. Magn. Mater. 226-230 (2001) 2081–2083.
[57] H. Bender, A. Van Esch, W. Van Roy, R. Oesterholt, J. De Boeck, G. Borghs, Structural characterization of InMnAs and GaMnAs epitaxial magnetic films grown by MBE on GaAs, IOP Publishing, 1995, pp. 293–296.
[58] H. Ohno, A. Shen, F. Matsukura, A. Oiwa, A. Endo, S. Katsumoto, Y. Iye, Appl. Phys. Lett. 69 (1996) 363–365.
[59] J. De Boeck, R. Oesterholt, A. Van Esch, H. Bender, B.C.C. Van Hoof, G. Borghs, Appl. Phys. Lett. 68 (1996) 2744.
[60] H. Shimuzu, et al., Appl. Phys. Lett. 74 (1999) 398.
[61] A. Shen, et al., Appl. Phys. Lett. 71 (1997) 1540.
[62] E. Matsukura, et al., Phys. Rev. B 57 (1998) 2037.
[63] T. Dietl, H. Ohno, F. Matsukura, J. Cibert, D. Ferrand, Science 287 (2000) 1019–1022.
[64] J. Koenig, H.-H. Lin, A.H. MacDonald, Phys. Rev. Lett. 84 (2000) 5628.
[65] A. Oiwa, et al., Physica B 249 (1998) 775.
[66] T. Omiya, et al., Physica E 7 (2000) 976.
[67] S. Von Molnar, et al., Phys. Rev. Lett. 51 (1983) 706.
[68] T. Story, et al., Phys. Rev. Lett. 56 (1986) 777.
[69] T. Dietl, A. Haury, Y. Merle d'Aubigne, Phys. Rev. B 55 (1997) R3347.
[70] C. Zener, Phys. Rev. 440 (299) (1950) 81–83.
[71] Z. Liu, V.V. Moshchalkov, G. Borghs, J. De Boeck (2001) in press.
[72] S. Datta, B. Das, Appl. Phys. Lett. 56 (1990) 665–667.
[73] R. Fiederling, M. Keim, G. Reuscher, W. Ossau, G. Schmidt, A. Waag, L.W. Molenkamp, Nature 402 (1999) 787–790.
[74] Y. Ohno, D.K. Young, B. Beschoten, F. Matsukura, H. Ohno, D.D. Awschalom, Nature 402 (1999) 790–792.
[75] G. Schmidt, D. Ferrand, L.W. Molenkamp, A.T. Filip, B.J. van Wees, Phys. Rev. B 62 (2000) R4790–R4793.
[76] F.G. Monzon, M.L. Roukes, J. Magn. Magn. Mater. 198-199 (1999) 632–635.
[77] A.T. Filip, B.H. Hoving, F.J. Jedema, B.J. van Wees, B. Dutta, G. Borghs, Phys. Rev. B 62 (2000) 9996–9999.
[78] E.I. Rashba, Phys. Rev. B 62 (2000) R16267–R16270.
[79] S.F. Alvarado, P. Renaud, Phys. Rev. Lett. 68 (1992) 1387–1390.
[80] S.F. Alvarado, Phys. Rev. Lett. 75 (1995) 513–516.

[81] C.J. Hill, X. Cartoixa, R.A. Beach, S.D.L., T.C. McGill, Cond-Mat/0010058 (2000).
[82] M.J.W. Prins, H. van Kempen, H. van Leuken, R.A. de Groot, W. Van Roy, J. De Boeck, J. Phys.: Condens. Matter 7 (1995) 9447–9464.
[83] V. Motsnyi, W. Van Roy, J. Das, E. Goovaerts, G. Borghs, J. De Boeck, in: Ferromagnetic Metal/Tunnel Barrier/Semiconductor Devices for Optical Detection of Spin-Polarized Current Injection into a Semiconductor, Grenoble, France (2001) submitted.
[84] H.J. Zhu, M. Ramsteiner, H. Kostial, M. Wassermeier, H.-P. Schonherr, Phys. Rev. Lett. 87 (2001) 016601.
[85] A. Hirohata, Y.B. Xu, C.M. Guertler, J.A.C. Bland, J. Appl. Phys. 87 (2000) 1–3.
[86] J.S. Moodera, L.R. Kinder, T.M. Wong, R. Meservey, Phys. Rev. Lett. 74 (1995) 3273–3276.
[87] J. De Boeck, G. Borghs, Phys. World 12 (1999) 27–32.
[88] K.-M.H. Lenssen, G.J.M. Dormans, R. Cuppens, "Expectations of MRAM in Comparison with Other Non-volatile Memory Technologies, Arlington, VA, USA, 2000.
[89] V.F. Motsnyi, V.I. Safarov, J. De Boeck, J. Das, W. Van Roy, E. Goovaerts, G. Borghs, Appl. Phys. Lett. (2002) in press.
[90] M. Tanaka, Y. Higo, J. Appl. Phys. 89 (2001) 6745–6747.
[91] Z. Liu, H. Boeve, W. Van Roy, S. Nemeth, V.V. Moshchalkov, G. Borghs, J. De Boeck, J. Cryst. Growth 227/228 (2001) 867–873.
[92] H. Ohno, D. Chiba, F. Matsukura, T. Omiya, E. Abe, T. Dietl, Y. Ohno, K. Ohtani, Nature 408 (2000) 944–946.
[93] M. Kohda, Y. Ohno, K. Takamura, F. Matsukura, H. Ohno, Jap. J. Appl. Phys. 40 (2001) 1274–1276.
[94] E. Johnston-Halperin, D. Lofgreen, R.K. Kawakami, D.K. Young, L. Coldren, A.C. Gossard, D.D. Awschalom, Phys. Rev. B 65 (2002) 041306.